Leukemia-associated RhoGEF (LARG) is a novel RhoGEF in cytokinesis and required for the proper completion of abscission

Matthew K. Martz[a], Elda Grabocka[a,*], Neil Beeharry[b], Timothy J. Yen[b], and Philip B. Wedegaertner[a]
[a]Department of Biochemistry and Molecular Biology, Thomas Jefferson University, Philadelphia, PA 19107; [b]Fox Chase Cancer Center, Philadelphia, PA 19111

ABSTRACT **Proper completion of mitosis requires the concerted effort of multiple RhoGEFs. Here we show that leukemia-associated RhoGEF (LARG), a RhoA-specific RGS-RhoGEF, is required for abscission, the final stage of cytokinesis, in which the intercellular membrane is cleaved between daughter cells. LARG colocalizes with α-tubulin at the spindle poles before localizing to the central spindle. During cytokinesis, LARG is condensed in the midbody, where it colocalizes with RhoA. HeLa cells depleted of LARG display apoptosis during cytokinesis with unresolved intercellular bridges, and rescue experiments show that expression of small interfering RNA–resistant LARG prevents this apoptosis. Moreover, live cell imaging of LARG-depleted cells reveals greatly delayed fission kinetics in abscission in which a population of cells with persistent bridges undergoes apoptosis; however, the delayed fission kinetics is rescued by Aurora-B inhibition. The formation of a Flemming body and thinning of microtubules in the intercellular bridge of cells depleted of LARG is consistent with a defect in late cytokinesis, just before the abscission event. In contrast to studies of other RhoGEFs, particularly Ect2 and GEF-H1, LARG depletion does not result in cytokinetic furrow regression nor does it affect internal mitotic timing. These results show that LARG is a novel and temporally distinct RhoGEF required for completion of abscission.**

Monitoring Editor
Francis A. Barr
University of Oxford

Received: Jul 20, 2012
Revised: Jul 2, 2013
Accepted: Jul 15, 2013

INTRODUCTION

Cytokinesis is the final stage of cellular division in which the cell is physically separated into two daughter cells. The mechanical act of partitioning the cytoplasm of the cell through ingression of the contractile ring to draw together membrane must be tightly coordinated with the segregation of genetic material. Failure to properly separate into daughter cells, or a miscue in timing between the completion of chromosomal segregation and doing so, can lead to tetraploidization of the cell, a phenomenon of genetic instability that has been shown to be beneficial to tumor formation (Fujiwara, 2005). A critical component of this spatiotemporal control involves the small GTPase RhoA, whose localization and activation are maintained by Rho guanine nucleotide exchange factors (RhoGEFs) and GTPase-activating proteins (RhoGAPs). It is through the regulation in the interplay between RhoGEFs and RhoGAPs that RhoA translocates to the equatorial cortex and initiates assembly and ingression of the contractile ring (Mishima *et al.*, 2002; Bement *et al.*, 2005; Yüce *et al.*, 2005; Su *et al.*, 2011a; Loria *et al.*, 2012).

A concert of RhoGEFs act during mitosis to ensure proper assembly and ingression of the cytokinetic furrow. MyoGEF has been shown to interact with the centrosome/spindle pole-associated protein (CSPP) and is necessary for recruitment of ECT2, RhoA, and nonmuscle myosin II to the central spindle (Asiedu *et al.*, 2009). ECT2 is recruited to the central spindle and equatorial cortex and is necessary for cortical localization and activation of RhoA, a critical step in the establishment of the cleavage furrow at the equatorial cortex (Tatsumoto *et al.*, 1999; Yüce *et al.*, 2005; Nishimura and Yonemura, 2006; Petronczki *et al.*, 2007; Wolfe *et al.*, 2009; Su *et al.*,

This article was published online ahead of print in MBoC in Press (http://www.molbiolcell.org/cgi/doi/10.1091/mbc.E12-07-0533) on July 24, 2013.

*Present address: Department of Biochemistry and Molecular Pharmacology, NYU Langone Medical Center, New York, NY 10016.

Address correspondence to: Philip Wedegaertner (philip.wedegaertner@jefferson.edu).

Abbreviations used: LARG, leukemia-associated RhoGEF; NS, nonspecific control siRNA; si, siRNA, small interfering RNA.

2011b). GEF-H1 was also shown to be important in directing the activation of RhoA during cleavage furrow ingression and may provide essential communication between the microtubule network responsible for segregating genomic material and the actomyosin-driven furrow ingression process (Krendel *et al.*, 2002; Birkenfeld *et al.*, 2007; Chang *et al.*, 2008; Fujishiro *et al.*, 2008). Of interest, studies have yet to uncover a role for a RhoGEF in the regulation of abscission, the fission of daughter cells after the completion of furrow ingression. Nonetheless, RhoGEFs have been shown to be localized in the dense midbody structure within the intercellular bridge formed from cytokinetic furrow ingression, suggesting a possible role post furrow ingression for RhoGEFs.

Leukemia-associated RhoGEF (LARG), also known as ARHGEF12, is a RhoA-specific RhoGEF first identified as a fusion product with MLL in acute myeloid leukemia; it remains one of the few RhoGEFs to be found mutated in human cancers (Fukuhara *et al.*, 2000). LARG is among a family of RhoGEFs activated by the $G\alpha_{12/13}$ G protein subunits and is also responsible for RhoA activation in signaling through a diversity of receptors, such as plexin-B1 (Aurandt *et al.*, 2002; Perrot *et al.*, 2002; Swiercz *et al.*, 2002), insulin-like growth factor-1 (Becknell *et al.*, 2003; Suzuki *et al.*, 2007), histamine-H1 (Pfreimer *et al.*, 2012), and sphingosine 1-phosphate receptor (Medlin *et al.*, 2010). Accordingly, LARG has been shown to be involved in cell polarization, cell morphology, and invasion (Swiercz *et al.*, 2002; Dubash *et al.*, 2007; Kitzing *et al.*, 2007; Goulimari *et al.*, 2008; Evelyn *et al.*, 2009; Shi *et al.*, 2009), including a report showing that LARG, along with GEF-H1, is critical in regulation of the mechanical response to force generated on integrins (Guilluy *et al.*, 2011).

Given the role of LARG in a multitude of mechanical transduction pathways, we sought to determine whether LARG is a member of the growing assemblage of RhoGEFs critical for proper mitotic regulation and dynamics. Here we show that LARG is indeed a novel mitotic RhoGEF displaying a distinct localization pattern with prominent midbody localization upon furrow ingression and during abscission. Depletion of LARG results in a late cytokinetic defect, and together these data show that LARG has a distinct functional significance from previously determined mitotic RhoGEFs during abscission.

RESULTS

Immunofluorescence staining of LARG in HeLa cells revealed a dynamic localization pattern through the cell cycle (Figure 1A). In interphase, LARG is predominantly found distributed evenly throughout the cytoplasm with a concentration colocalizing with α-tubulin at the microtubule-organizing center (MTOC), similar to localization patterns previously identified for LARG (Goulimari *et al.*, 2008). On initiation of mitosis and through early anaphase, LARG colocalizes with α-tubulin at the spindle poles and along microtubule tracks, as well as at the centrosomes. During late anaphase, before initiation of contractile ring ingression, LARG localizes to the spindle midzone. We did not find LARG localized at the cortex of the contractile ring, where ECT2 is known to concentrate just before initiation of ingression (Yüce *et al.*, 2005). Finally, during telophase and cytokinesis, LARG is prominently localized within the intercellular bridge at the midbody, or Flemming body, the dense structure formed from the collapse of the spindle midzone. Strong midbody localization of LARG was also observed in noncancerous, immortalized RPE-1 cells (Supplemental Figure S1A), detected by multiple antibodies in HeLa cells (Supplemental Figure S1B), and lost on small interfering RNA (siRNA) depletion of LARG in HeLa cells (Supplemental Figure S1, C and D). RhoA concentrates at the cell cortex before contractile ring ingression before condensing in the midbody during cytokinesis (Nishimura and Yonemura, 2006; Yonemura *et al.*, 2004). Of interest, it is not until after full contractile ring ingression that LARG is observed to colocalize with RhoA (Figure 1B). Taken together, these

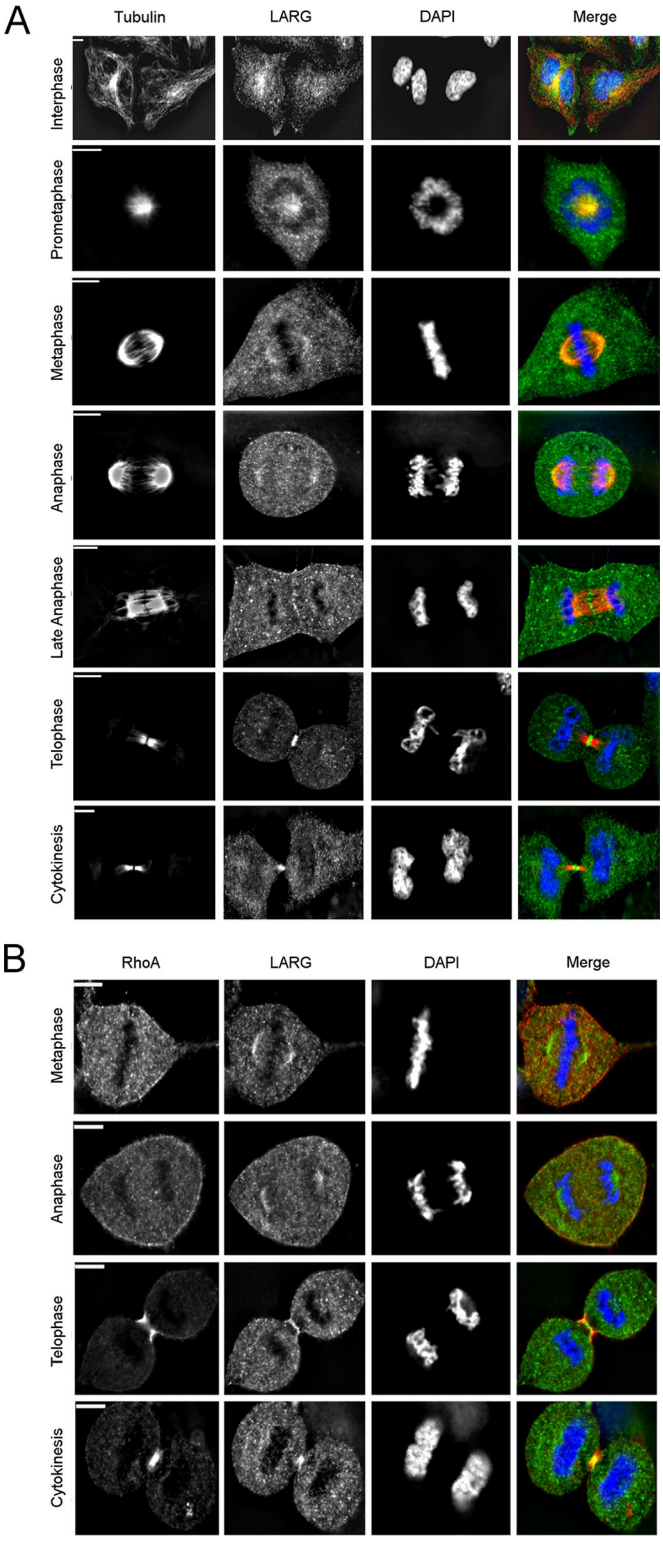

FIGURE 1: Mitotic distribution of LARG. (A, B) HeLa cells were fixed, and α-tubulin (red), RhoA (red), LARG (green; SC H70), and DNA (blue) were visualized by immunofluorescence microscopy, as described in *Materials and Methods*. Bar, 11 μm.

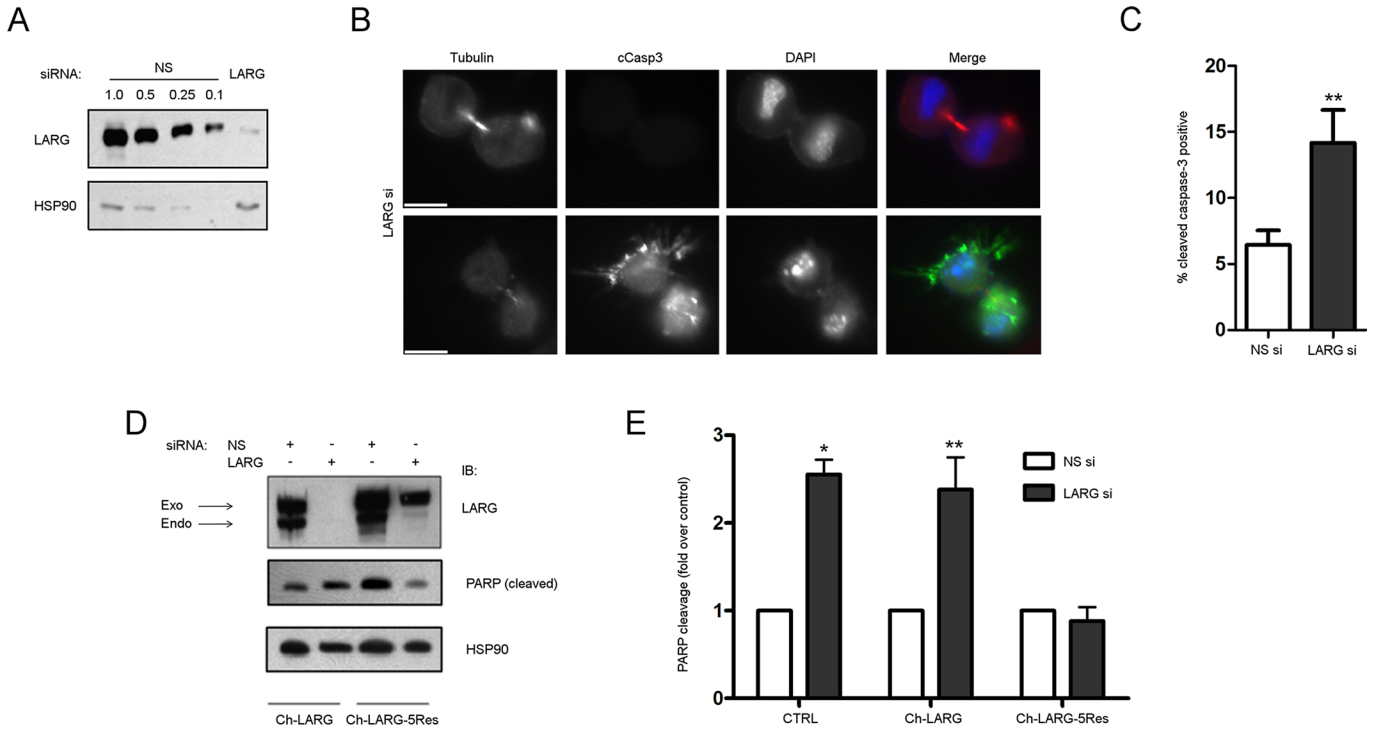

FIGURE 2: Depletion of LARG results in apoptosis. (A) HeLa cells were treated with non- NS or LARG siRNA as described in *Materials and Methods*. Efficiency of endogenous LARG depletion (>90%) is shown by an immunoblot of cell lysates comparing the LARG signal in LARG siRNA lysates to decreasing equivalents of NS cell lysates. (B) HeLa cells were treated with LARG siRNA and fixed 12 h after release from double-thymidine G1/S synchronization to enrich for cells undergoing mitosis. Cells were stained for α-tubulin (red), cleaved caspase-3 (green), and DNA (blue). Images show examples of normal (top) and apoptotic (bottom) cytokinesis in LARG siRNA–treated cells. Bar, 10 μm. (C) Quantification of the percentage of cleaved caspase-3–positive cells (**$p < 0.05$, $n = 1438$ NS si cells, 1021 LARG si cells). (D) HeLa cells were transfected with the indicated siRNA together with expression plasmids for mCherry-LARG (Ch-LARG) or the siRNA-resistant Ch-LARG-5Res and analyzed by immunoblot for PARP-1 cleavage as described in *Materials and Methods*. The arrows indicate the position of endogenous LARG (endo) and exogenous mCherry-tagged LARG (exo). (E) Quantification of PARP-1 cleavage as fold change over control siRNA–treated cells normalized for HSP90 loading control (*$p = 0.0008$, **$p < 0.02$, $n = 3$ independent experiments).

localization data suggested that LARG may hold functional significance in the midbody after complete furrow ingression during abscission, a novel role both for LARG and for a RhoGEF.

To assess whether the localization of LARG correlated with some aspects of mitotic progression, we depleted HeLa cells of LARG using siRNA (LARG si; using siRNA #5 as described in *Materials and Methods*) and sought to identify any potential mitotic defects (Figure 2A). Of interest, we noted a population of LARG si cells connected by intercellular bridges with distinct cell death morphologies (Figure 2B). Cells were often found in tandem with drastic membrane disorganization and pyknosis of the nuclei while attached by a membranous extension that contained microtubule bundles, hallmark indications of active apoptosis (Kerr *et al.*, 1972). To confirm that the morphological changes we observed in LARG si cells were due to apoptosis, we stained nonspecific siRNA–treated (NS) and LARG si cells with an antibody targeted against the cleaved form of caspase-3. This staining revealed that LARG si cells displaying severe morphological changes were positive for cleaved caspase-3 and indeed undergoing apoptosis (Figure 2, B and C). In addition, increased poly[ADP-ribose] polymerase (PARP) cleavage, another hallmark of apoptosis (Slee *et al.*, 2001), was observed in immunoblots of cell lysates from LARG si cells (Figure 2, D and E). We further confirmed these data with additional siRNAs targeting LARG in both pool and individual forms (data not shown). Of importance, the increased apoptosis in LARG si cells was alleviated by introduction of an siRNA-resistant, mCherry-tagged LARG (Figure 2, D and E). Thus, on the basis of these observations of increased apoptosis and apoptotic cells connected by intercellular bridges after LARG depletion, we postulated that LARG was required for both cell viability and mitotic progression.

To better understand where in mitosis LARG was functionally required, we monitored division by live cell microscopy of HeLa cells stably expressing green fluorescent protein (GFP)–H2B (Kanda *et al.*, 1998; Figure 3 and Supplemental Videos S1 and S2). LARG si cells proceed through early mitosis without any notable error, such as chromosomal missegregation, chromatin bridges, spindle defects, or alteration of early mitotic kinetics, as noted by monitoring hallmark chromatin changes during mitosis. Moreover, fixing a parallel set of LARG si cells just before or after filming, followed by staining for γ-H2AX (Yang, 2008), revealed no evidence of DNA damage (data not shown). That we could not detect any decoration of DNA with staining for γ-H2AX is further confirmation that depletion of LARG does not affect chromosome integrity or segregation dynamics.

Depletion of MyoGEF or ECT2 leads to contractile ring assembly and ingression phenotypes (Tatsumoto *et al.*, 1999; Yüce *et al.*, 2005; Nishimura and Yonemura, 2006; Wu *et al.*, 2006; Petronczki *et al.*, 2007; Asiedu *et al.*, 2009; Wolfe *et al.*, 2009; Su *et al.*, 2011b).

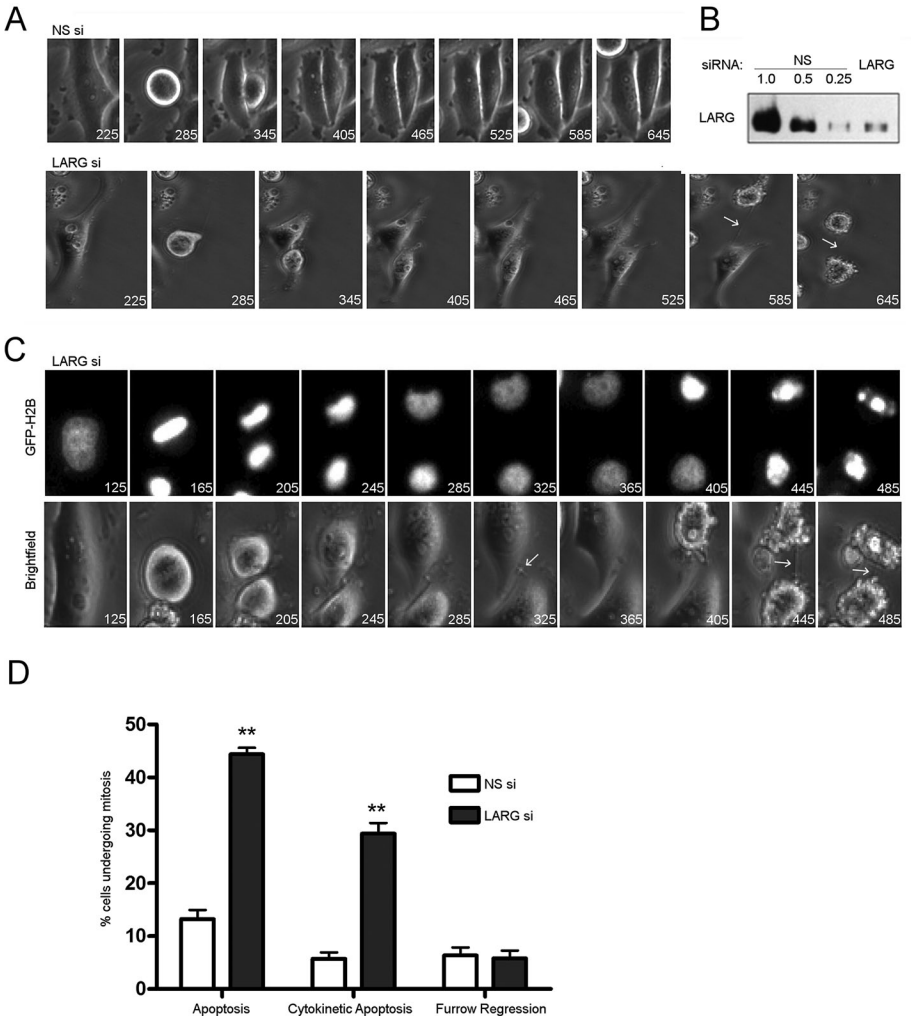

FIGURE 3: Depletion of LARG results in apoptosis in late cytokinesis. HeLa cells stably expressing GFP-H2B were treated with the indicated siRNA and synchronized at G1/S by the double-thymidine method. Cells were released from G1/S block and imaged by live cell microscopy with times indicated in minutes. (A) Bright-field images of cells progressing through mitosis after treatment with indicated siRNAs. Arrows highlight intercellular bridge in LARG si–treated cells. (B) Representative Western blot of the depletion of LARG in imaged cells. (C) GFP-H2B and bright-field images of LARG si–treated cells showing the classic degradation of DNA and membrane blebbing indicative of apoptosis after unresolved cytokinesis. Arrows highlight intercellular bridges. (D) Quantification of fates of NS and LARG si–treated cells that enter mitosis. Values expressed as a percentage of total number of cells entering mitosis during filming (**$p < 0.0005$, $n = 262$ NS si cells, 297 LARG si cells across three independent experiments).

These range from an inability to properly assemble the contractile ring at the cell cortex to instability and perturbation of the ingression forces. The net result is the regression of the forming cytokinetic furrow to form a binucleate cell. GEF-H1 depletion results in a more variable phenotype but also ultimately yields incomplete furrow formation and polyploidy (Birkenfeld, 2007). Somewhat surprisingly, unlike depletion of other mitotic RhoGEFs, LARG si cells can initiate contractile ring assembly and ingression without any noticeable perturbations. This is followed by an unremarkable completion of furrow ingression to form a stable intercellular bridge and dense midbody structure just before abscission (Figure 3A and Supplemental Video S2).

A difference arose, however, in late cytokinesis. LARG si cells were unable to complete the final fission step. Thus daughter cells remained connected by the membranous intercellular bridge. The postingression midbody remained dense and seemingly well formed but underwent no further progression toward abscission. Of interest, we observed that a subpopulation of LARG si cells stuck in this late cytokinesis further underwent apoptosis (Figure 3, A and C). GFP-H2B in this subpopulation formed aggregates that were indicative of apoptosis (Figure 3C and Supplemental Video S3). Of LARG si cells going through mitosis, 44% of them died through apoptosis, a threefold increase over control NS si cells. Moreover, when specifically examining cells in late cytokinesis, LARG si cells showed a fivefold increase in apoptosis compared with control NS si cells (Figure 3, C and D, and Supplemental Video S4). Of note, LARG si cells spend approximately twice as long in late cytokinesis as control cells, as described later (Figure 4). To account for these altered kinetics, we normalized mitotic apoptosis by time spent in preingression and postingression stages (Supplemental Figure S2). Overall, LARG si cells display a twofold increase in time-normalized, mitotic apoptosis. Precytokinesis also represents a twofold increase in apoptosis, a stage in which there is no difference in time between LARG and NS si cells. On the other hand LARG si cells display a 2.5-fold increase in late cytokinetic apoptosis over NS si cells. Although LARG si cells show a trend toward increased time-normalized apoptosis in cytokinesis as compared to control cells, we have been unable to clearly show significance here. Thus it remains to be completely resolved whether these two phenotypes—increased apoptosis and delayed abscission—that are observed upon LARG depletion are distinct or causally linked.

Introduction of the pancaspase inhibitor Z-VAD-FMK prevented abscission-related apoptosis, and persistent intercellular bridges between daughter cells could often be visualized for the length of filming (Supplemental Figure S3). That LARG si cells show full contractile ring ingression but have a significant population that undergoes apoptosis during abscission is a unique phenotype among the mitotic RhoGEFs and suggests an essential role for LARG in abscission.

To determine at what stage in the late cytokinetic program LARG si cells become defective, we monitored HeLa cells stably expressing GFP-tubulin by live cell microscopy (Figure 4). Microtubules undergo several distinct structural changes during the collapse of the cytokinetic furrow and resolution of the intercellular bridge through abscission (Fededa and Gerlich, 2012). Dense, overlapping microtubules form at the spindle midzone during anaphase and become compressed in the cytokinetic furrow during contractile ring ingression. During late cytokinesis, just before abscission, microtubules undergo thinning in the intercellular bridge, overlap in the midbody,

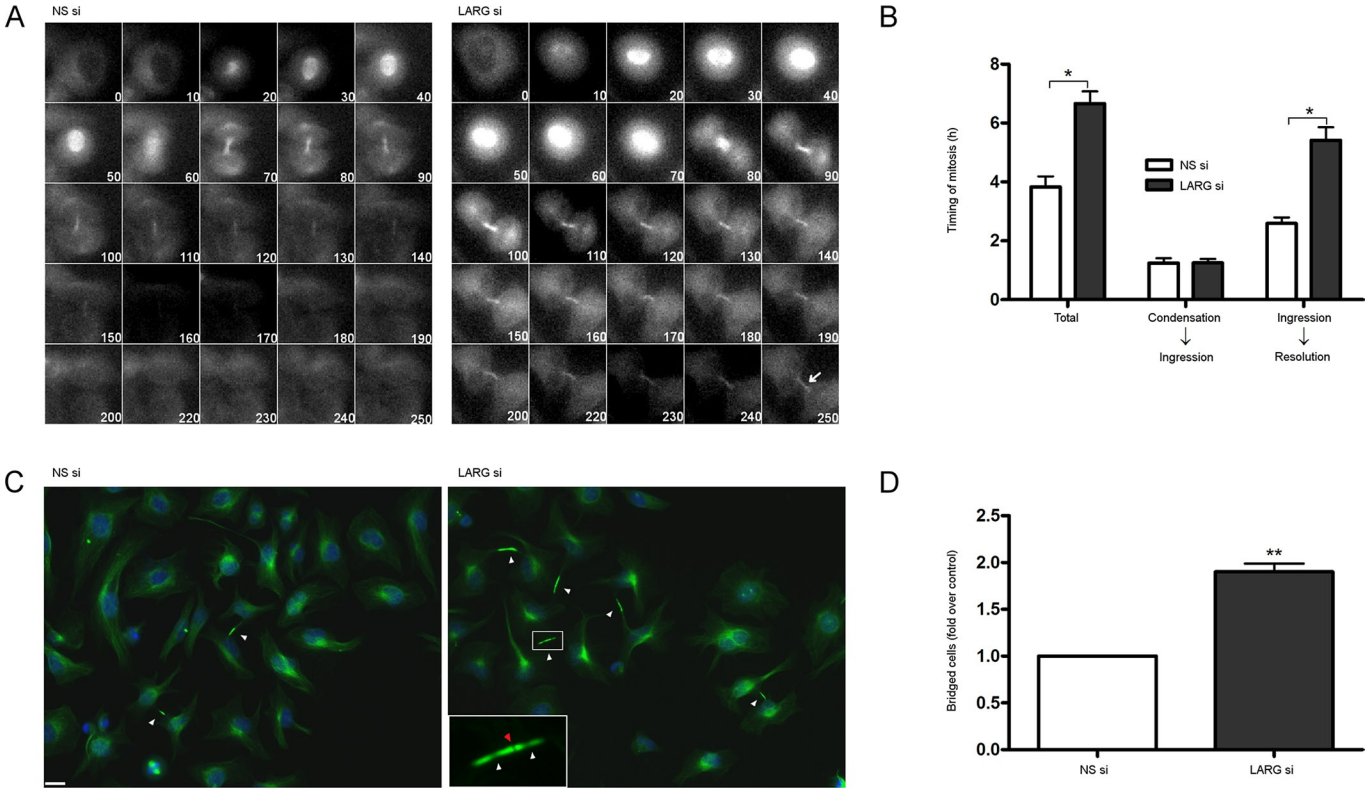

FIGURE 4: Cells depleted of LARG undergo normal mitotic kinetics but are unable to complete abscission. (A) HeLa cells stably expressing GFP–α-tubulin were treated with the indicated siRNA, synchronized at G1/S by the double-thymidine method, and imaged by live cell microscopy beginning just before initiation of mitosis (times indicated in minutes). Arrow highlights presence of α-tubulin in LARG si cells well after control NS si cells have completed abscission. (B) Quantification of mitotic kinetics as measured by α-tubulin dynamics (*$p < 0.0001$, $n = 97$ NS si cells, $n = 85$ LARG si cells). Total, initiation of mitosis to intercellular α-tubulin resolution; condensation to ingression, initiation of mitosis to completion of contractile ring ingression; ingression to resolution, completion of contractile ring ingression to intercellular α-tubulin resolution. (C) HeLa cells were treated with siRNA, fixed 12 h after release from double thymidine, and stained for α-tubulin (green) and DNA (blue). Arrows highlight intercellular bridges that have completed contractile ring ingression. LARG si inset highlights Flemming body with proper midbody matrix (red arrow) and distal thinning of microtubules in the intercellular bridge (flanking white arrows). Bar, 10 μm. (D) Quantification of cells connected by persistent α-tubulin–containing intercellular bridges as fold over control NS si cells (**$p < 0.0005$, $n \geq 1500$ cells for each siRNA across three independent experiments).

and form sites of secondary ingression before being severed just before fission.

As with data obtained from tracking chromosomal dynamics (Figure 3), LARG si cells are able to proceed through early mitosis with comparable kinetics to control siRNA–transfected cells. We observed a significant difference between LARG si and NS si cells upon completion of furrow ingression and narrowing of tubulin in the intercellular bridge; LARG si cells display a twofold increase in the time to detect loss of GFP-tubulin signal from the intercellular bridge, (5.4 vs. 2.6 h in NS si cells), indicative of a defect in abscission or the molecular events immediately preceding abscission rather than earlier during contractile ring ingression (Figure 4, A and B). We noted that a population of LARG si cells never resolved tubulin from the intercellular bridge before completion of filming (9 vs. 2% in NS si cells) and others that went through apparent forced abscission events due to mechanical shearing of the intercellular bridge.

The inability of LARG si cells to complete abscission results in an accumulation of G1-like cells that remain connected by tubulin-containing intercellular bridges (Supplemental Figure S4). This is evidence that in the absence of abscission, cells are still able to undergo subsequent rounds of mitosis. Similar multicellular intercellular bridge accumulation has been seen in other studies of late cytokinetic proteins and complexes, such as Sept9, exocyst complex, and rab35 GTPase (Gromley, 2005; Estey *et al.*, 2010; Dambournet *et al.*, 2011).

To achieve higher resolution of the microtubules comprising the intercellular bridge and detect potential structural abnormalities, we analyzed postmitotic fixed cells. Cells were either depleted of LARG or treated with nonspecific control siRNA, synchronized at G1/S by the double-thymidine method, released by washout, and allowed to proceed through mitosis. Cells were then fixed 10–12 h postrelease, when most cells should have completed abscission. Midbody-stage cells were scored as those with intercellular bridges comprising a thin microtubule network with a midbody that excluded α-tubulin antibody due to its dense matrix. LARG si cells displayed a twofold to threefold increase in persistent, midbody-stage intercellular bridges (Figure 4, C and D). We further noted that LARG si cells formed stable midbody bulges displaying hallmark α-tubulin antibody exclusion, as well as distal thinning of microtubules in the intercellular bridge (Mullins and Biesele, 1977; Steigemann and Gerlich, 2009; Figure 4C, inset).

These data suggest that LARG si cells form a proper midbody matrix and can assemble the primary abscission machinery but are unable to complete downstream fission events (Matuliene and Kuriyama, 2002; Elia *et al.*, 2011). Moreover, apoptosis in LARG si cells (4–5 h post mitotic initiation) occurs after the time required for normal completion of cytokinesis and abscission in control NS si cells (3–4 h post mitotic initiation, as detected by resolution of GFP-tubulin from the intercellular bridge). These observations are consistent with the idea that depletion of LARG causes a defect in late cytokinesis just before abscission, in which a subpopulation of cells has an increased propensity for apoptosis (Figures 4B and 3, A and B). We further analyzed the localization of several well-characterized midbody-associated proteins, including ECT2, TSG101, Aurora-B, Plk1, RhoA, and Mklp1, and found them to all be properly localized in LARG si cells (Supplemental Figure S5). With the observed maturity of LARG si intercellular bridges, it was not surprising to find that interrogated midbody and abscission machinery components were in well order. Together the data in Figure 4 are consistent with our hypothesis that LARG is necessary in the very late stages of cytokinesis for the timely completion of abscission.

To begin to address a mechanism by which depletion of LARG causes a delay in late cytokinesis, we examined whether inhibition of Aurora-B could bypass the delay. Aurora-B kinase is important not only in early mitotic dynamics, but also in cytokinesis (Eggert *et al.*, 2006). Both Aurora-B and the budding yeast homologue Ipl1 control an abscission checkpoint in the presence of chromosomal segregation errors. Incomplete clearance of chromosomal material from the intercellular bridge results in sustained Aurora-B activity and stabilization of the bridge, preventing abscission (Norden *et al.*, 2006; Steigemann *et al.*, 2009). Moreover, inhibition of Aurora-B activity is sufficient to relieve the abscission checkpoint in the presence of nuclear pore formation perturbations (Mackay *et al.*, 2010). Here asynchronous siRNA-transfected cells were treated with 2 μM ZM447439, a small-molecule inhibitor of Aurora-B, or dimethyl sulfoxide (DMSO) vehicle for 2 h before fixation. With vehicle treatment, LARG si cells displayed typical increase in persistent intercellular bridges compared to NS si cells (Figure 5, A–C). On inhibition of Aurora-B, however, in both LARG and NS cells we observed a significant decrease in the number of midbody stage cells (Figure 5B). Of importance, LARG si displayed a significant decrease in the number of midbody stage cells even when normalized for the decrease observed with NS si cells (Figure 5C), suggesting that Aurora-B activity mediates delayed abscission kinetics in the absence of LARG. We noted no distinguishable increase in binucleate cell formation between NS and LARG si cells, indicating that the resolution of intercellular bridges in LARG si cells when treated with ZM447439 was not due to regression of the cytokinetic furrow. In addition, immunofluorescence with an Aurora-B antibody and phospho-specific Aurora-B antibody to detect active Aurora-B showed midbody localization in NS si and LARG si cells (Supplemental Figure S5), consistent with a role for Aurora-B in mediating delayed abscission upon LARG depletion.

Finally, by generating a mutant LARG deficient in RhoA activation, we attempted to examine whether the role of LARG in delayed abscission and apoptosis requires its canonical activation of RhoA. To generate such a mutant, we tested several different single–amino acid substitutions, based on previous biochemical and structural data (Figure 6C; Kristelly *et al.*, 2003; Aittaleb *et al.*, 2009) and assayed for loss of interaction with RhoA-G17A, a nucleotide-empty form of RhoA. The ability of glutathione *S*-transferase (GST)–RhoG17A to pull down LARG from cell lysates is a convenient assay for detecting LARG that is active in terms of RhoGEF activity (Garcia-Mata

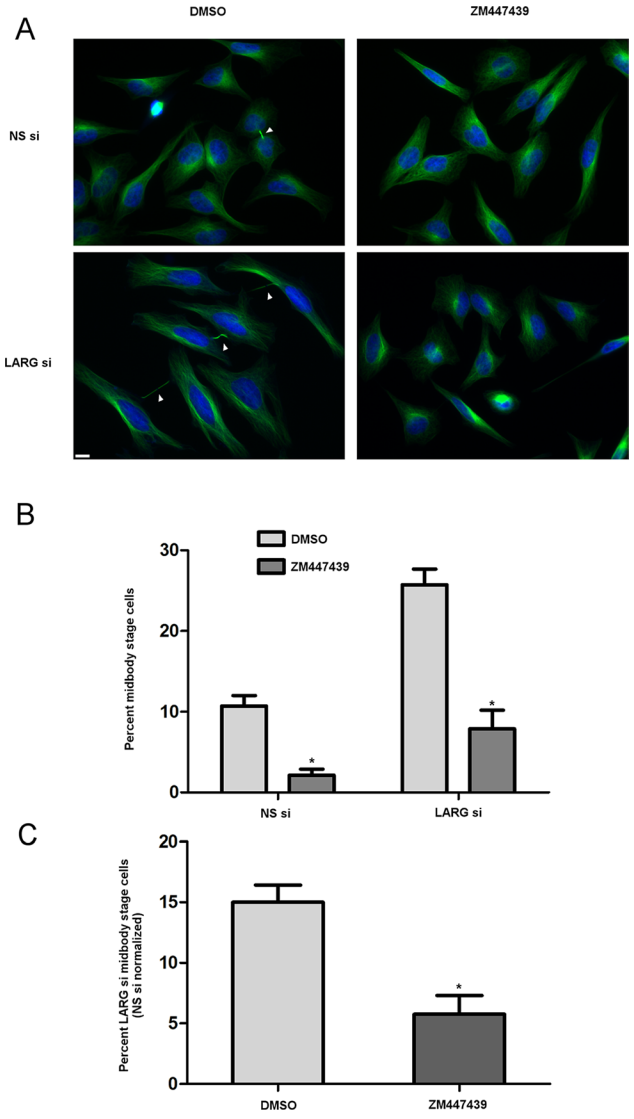

FIGURE 5: Cells depleted of LARG undergo an Aurora-B–dependent delay in abscission kinetics. (A) Asynchronous HeLa cells were treated with siRNA for 72 h. Cells were treated with either DMSO vehicle or 2 μM ZM447439 to inhibit Aurora-B for 2 h before fixing and staining for α-tubulin (green) and DNA (blue). Arrows highlight midbody-stage intercellular bridges. Bar, 10 μm. (B) Quantification of the percentage of midbody-stage intercellular bridges for both NS si and LARG si cells in the presence of vehicle or Aurora-B inhibitor (*$p \leq 0.0012$, DMSO vs. ZM447439; DMSO, NS si = 7478 cells, LARG si = 3388 cells; ZM447439, NS si = 7229 cells, LARG si = 4249 cells; across four independent experiments). (C) Percentage of midbody-stage intercellular bridges for LARG si cells normalized by subtraction of NS si cell percentages for each DMSO and ZM447439 treatment (*$p = 0.0045$).

et al., 2006). The LARG-W769A mutant showed a fivefold decrease in pull down with GST-Rho-G17A compared to wild-type (WT) transfected LARG, whereas the LARG-E790A mutant surprisingly retained interaction with GST-Rho-G17A (Figure 6A). The LARG-Y940A mutant, however, was completely unable to be pulled down by GST-Rho-G17A (Figure 6A), identifying this mutant as a LARG that is incapable of activating RhoA. In our preliminary studies of LARG-Y940A, we noted that it was difficult to detect its expression. Of interest, we further noted a drastic decrease in viability in cells transiently

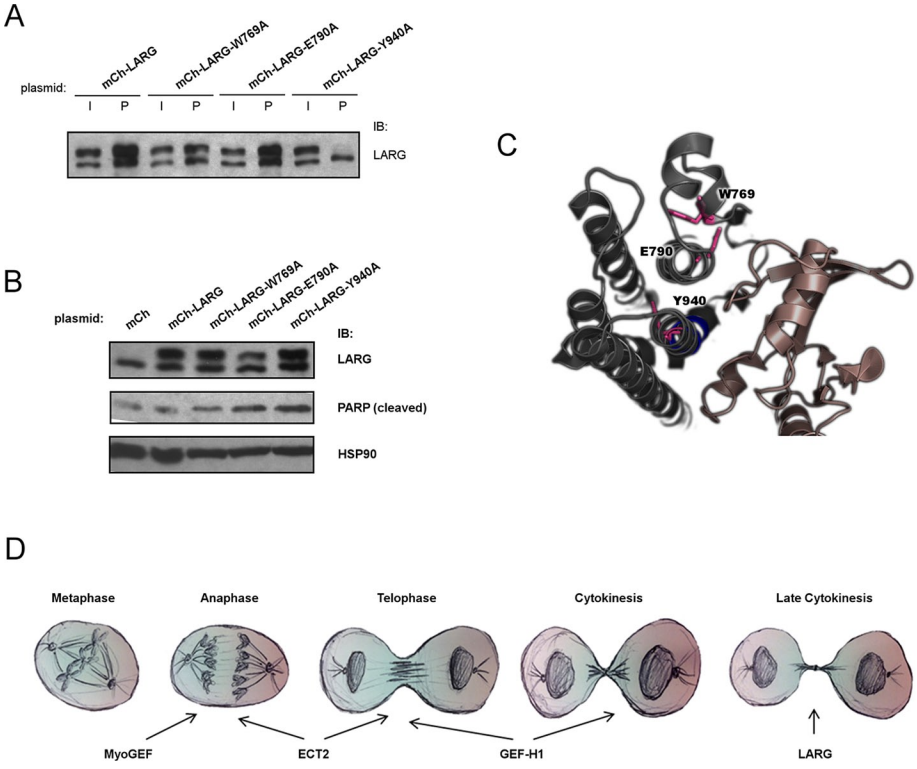

FIGURE 6: Y940 of the DH core of LARG is critical for binding to RhoA, and mutation leads to apoptosis. (A) HeLa cells were transfected with indicated plasmid. At 48 h posttransfection, cell lysates were harvested and subject to GST-G17A-RhoA pull down. Relative binding to RhoA was determined by immunoblot for LARG and pull down and input fractions compared for each respective LARG plasmid. I, 5% total input; P, 50% total pull down. Top bands, exogenous mCherry-tagged LARG proteins; bottom bands, endogenous LARG. (B) HeLa cells were transfected with indicated plasmid for 48 h, cell lysates harvested, and relative apoptosis determined by immunoblot for PARP cleavage. (C) Crystal structure of DH/PH domain of LARG in complex with RhoA from PDB database (1X86; Kristelly *et al.*, 2003) depicting residues (pink) of the DH domain (gray) targeted here in mutation studies and relative locations to RhoA (brown). (D) Multiple RhoGEFs exhibit temporally distinct functions for the proper completion of mitosis. See the text for discussion.

overexpressing this mutant compared to WT LARG. This led us to hypothesize that LARG-Y940A, which cannot bind to RhoA, causes apoptosis in a dominant-negative manner. Indeed, we observed increased PARP cleavage with overexpression of LARG-Y940A (Figure 6B). Surprisingly, we also observed increased apoptosis in cells expressing LARG-E790A and, to a lesser degree, LARG-W769A. These observations of increased apoptosis upon expression of RhoGEF activity–deficient LARG suggest that LARG-Y940A, and possibly the other mutants, are functioning in a dominant-negative manner and thus are consistent with our results here using siRNA depletion of LARG. Further, these data suggest that RhoA activation is required for LARG's role in maintaining cell viability and, by extension, LARG's role in late cytokinesis. We were unable to directly test this; the fact that LARG-Y940A promotes apoptosis prevented us from using it in siRNA rescue experiments and makes it technically challenging to identify late-cytokinesis cells expressing this mutant of LARG.

DISCUSSION

The studies presented here show a novel and specific role for LARG in cytokinesis. Depletion of previously identified mitotic RhoGEFs results in cytokinetic defects ranging from the inability to properly initiate contractile ring ingression to cortical instability and failure to fully ingress and form the cytokinetic furrow (Tatsumoto *et al.*, 1999; Wu *et al.*, 2006; Birkenfeld, 2007; Su *et al.*, 2011b). Depletion of LARG arrests the abscission process, resulting in cells that have completed contractile ring ingression but remain unable to complete abscission with proper kinetics, a temporally distinct requirement from previously identified mitotic RhoGEFs (Figure 6D). The presence of Flemming bodies with proper midbody matrix formation in LARG si cells suggests that cells are able to complete ingression and begin the proper localization of endosomal-derived components and abscission machinery but are unable to proceed forward to sever microtubules and begin the final fission event (Elia *et al.*, 2011; Neto and Gould, 2011). Moreover, we noted a subpopulation of LARG si cells with an increased propensity for apoptosis while arrested in late cytokinesis.

Work on an Aurora-B–controlled checkpoint in abscission (Mackay *et al.*, 2010; Steigemann, 2009) suggests that the cellular sampling algorithm used to monitor abscission and drive the final outcome of mitotic division is not merely mechanical in nature but involves multiplexed signaling cascades. Our result showing that treatment of LARG si cells with an Aurora-B inhibitor allows cells to bypass the delay in abscission suggests that Aurora-B plays an active role in the observed delayed kinetics. Not only is this exciting in that it uncovers a likely mechanistic pathway responsible for delayed abscission kinetics when LARG is depleted from cells, it also reveals a novel insight into cytokinetic regulation. The Aurora-B abscission checkpoint pathway has been believed to be chromatin dependent and target the clearance of genetic material from the intercellular bridge, although additional work suggests that this checkpoint is also activated when nuclear pores are not reformed properly (Mackay *et al.*, 2010). We showed that depletion of LARG does not disrupt normal chromosomal segregation fidelity. Yet, when LARG is absent, cells are unable to satisfy the Aurora-B–mediated abscission checkpoint. Thus our results propose a nuclear- and chromatin-independent mechanism of sustained checkpoint activity. These data suggest a more omnipotent abscission checkpoint, one that ensures not only proper completion of cytokinesis in monitoring chromosomal clearance, but also a multitude of convergent mechanical and biochemical signaling pathways.

LARG is not the first regulator of cytokinesis or abscission whose disruption results in apoptosis; however, LARG and GEF-H1 appear to be exclusive as RhoGEFs whose cytokinetic impairment can result in cell death (Tomas, 2004; Birkenfeld, 2007; Pohl and Jentsch, 2008; Estey *et al.*, 2010). Outcomes in which daughter cells are not properly separated result in a state of cellular aneuploidy, genetic instability beneficial for tumor formation and growth, as well as increased susceptibility to transformation after carcinogenic exposure (Fujiwara, 2005). A common therapeutic approach for targeting mitotic cells is to use antispindle agents, such as vinca alkaloids and taxanes. However, populations of cells can undergo slippage out of

this block, continuing mitotic division and thus proliferating with potentially increased genetic instability (Rieder and Palazzo, 1992; Di Leonardo *et al.*, 1997; Tao *et al.*, 2005). Therefore proteins that regulate processes downstream of spindle assembly, such as mitotic exit, provide alternative anticancer targets (Huang *et al.*, 2009). LARG and other proteins whose disruption likewise results in apoptosis during failed abscission rather than furrow regression and aneuploidy pose therapeutically enticing targets. One important question that remains to be answered is exactly how and when apoptosis is being triggered. Further, it is not understood whether the cytokinetic defect and resultant delay may be causing apoptosis and, if so, the mechanistic derivation of this signal. Finally, although siRNA-resistant LARG could rescue the increased apoptosis caused by LARG depletion, we could not consistently observe overexpressed LARG at the midbody. Thus it remains unresolved whether midbody localization of LARG is essential for its antiapoptotic function.

RhoGEFs identified as necessary for mitosis have proven to be critical for the proper assembly, constriction, and stability of the contractile ring. There appear to be, however, no previously shown postingression phenotypes during late cytokinesis and subsequent abscission when these RhoGEFs are siRNA depleted. This posed the intriguing question as to whether regulation of RhoA activity is a crucial step in late cytokinesis and, correlatively, if there is a functionally relevant RhoGEF after complete contractile ring ingression necessary for the completion of abscission. Recent work revealed a role for citron kinase (CIT-K) upstream of RhoA at the midbody stage of cytokinesis (Gai *et al.*, 2011). Overexpression of CIT-K results in increase in active RhoA in late cytokinesis, leading to abscission delay that can be rescued by inactivation of RhoA by C3-toxin. Conversely, depletion of CIT-K results in significant reduction of active RhoA in late cytokinesis and, of interest, reduction in the total RhoGEF activity at this stage. It was noted, however, that no disruption in localization or activity of the canonical mitotic RhoGEFs ECT2 and GEF-H1 or RhoGAPs p190RhoGAP and RACGAP1 could be observed with CIT-K depletion. Therefore it is likely that the CIT-K and RhoA pathway in late cytokinesis is connected to a yet-unfound mitotic RhoGEF. Given that depletion of LARG from cells results in an abscission delay and sustained Aurora-B checkpoint activity, it is a rather fitting candidate for such a role. It will therefore be exciting to determine the late cytokinetic interactome of LARG and whether it is indeed cooperating with CIT-K to control the activity and stable localization of RhoA just before abscission.

Mutational analysis of LARG DH–domain residues showed that Y940 is critical for binding to RhoA and, further, that LARG-Y940A appears to act in a dominant-negative manner, ultimately causing apoptosis. Cells depleted of LARG have a high propensity for abscission-related apoptosis while attempting to undergo cytokinesis. Given that overexpression of LARG-Y940A, which is completely unable to bind RhoA, also results in apoptosis, we hypothesize that these are related phenotypes and that LARG binding to RhoA is important for cell viability. We anticipate that this regulation of RhoA activity is critical for proper late cytokinesis and abscission kinetics and, ultimately, viability in cytokinesis. Further experimentation is needed, however, to confirm that these are interconnected phenomena. Further studies should elucidate with finer detail the temporal requirement for LARG in abscission and whether there is a functional requirement for discrete RhoA activation during certain events in the abscission process after completion of contractile ring ingression.

In summary, this study shows that depletion of LARG causes a delay in late cytokinesis and thus provides evidence for an unexpected mitotic role for LARG. Further understanding of the molecular requirement for LARG in late cytokinesis should provide crucial insight into the upstream modalities of abscission regulation.

MATERIALS AND METHODS

Cell culture, plasmids, and transfections

Cell lines were cultured in either DMEM (HeLa) or 50:50 DMEM:F12 (RPE1) with 10% fetal bovine serum at 37°C and 5% CO_2. mCherry-LARG (Ch-LARG) was constructed as previously described (Grabocka and Wedegaertner, 2007). Cells were transfected in six-well plates with HiPerFect (Qiagen, Valencia, CA) for siRNA or Lipofectamine 2000 (Invitrogen, Carlsbad, CA) for siRNA and plasmid cotransfection. For siRNA depletion experiments, cells were transfected with either NS control siRNA (D-001810-01) or those targeted against LARG, ARHGEF12 siGenome ON-TARGET plus set (J-008480; Dharmacon, Lafayette, CO), at 50 nM concentration using the manufacturer's instructions. LARG siRNA #5 was used for further single-siRNA studies (J-008480-05, GAUCAAAUCUCGUCAGAAA). Cells were then harvested 48–72 h later unless otherwise noted. siRNA resistance (Ch-LARG-5res) was generated by introduction of silent mutations into the LARG siRNA #5 binding sequence of Ch-LARG by QuikChange mutagenesis (GATCAAAAGTCGTCAGAAA). DH-domain mutants were constructed by QuikChange PCR mutagenesis of W769 (mCh-LARG-W769A), E790 (mCh-LARG-E790A), or Y940 (mCh-LARG-Y940A) to alanine in mCherry-LARG (Ch-LARG).

Immunoblotting

Cells were lysed and subjected to standard immunoblotting procedures using overnight incubation of primary antibodies with 1 h of secondary antibody incubation. Primary antibody dilutions were anti-LARG, 1:2000 (goat RD AF4737, R&D Systems, Minneapolis, MN; rabbit A301-959A, Bethyl Laboratories, Montgomery, TX; rabbit H70, Santa Cruz Biotechnology, Santa Cruz Biotechnology, CA); rabbit anti-PARP1, 1:2000 (Santa Cruz Biotechnology); mouse anti–α-tubulin, 1:2000 (DM1A; Sigma-Aldrich, St. Louis, MO); and rabbit anti-HSP90 α/β, 1:25,000 (Santa Cruz Biotechnology). Secondary antibody coupled to horseradish peroxidase was used at 1:10,000 (Promega, Madison, WI). Densitometry of Western blots was performed using Quantity-One (Bio-Rad, Hercules, CA).

Immunofluorescence

Cells were washed with phosphate-buffered saline and fixed in either 10% trichloroacetic acid at 4°C for 10 min or 3.7% paraformaldehyde at 24°C for 15 min. Cells were then permeabilized by blocking in 1% Triton X-100 in Tris-buffered saline containing 2.5% nonfat milk or bovine serum albumin. Primary antibodies were incubated for 1.5 h and secondary antibodies for 0.5 h. Primary antibody dilutions were anti-LARG, 1:1000 (goat RD AF4737, R&D Systems; rabbit A301-959A, Bethyl Laboratories; rabbit H70, Santa Cruz Biotechnology); rabbit anti–cleaved caspase-3, 1:1000 (Cell Signaling Technology, Beverly, MA); mouse anti-RhoA, 1:500 (sc-179, Santa Cruz Biotechnology); rabbit anti-MKLP-1 (N-19, Santa Cruz Biotechnology), mouse anti-TSG101 (ab83; Abcam, Cambridge, MA), rabbit anti-ECT2 (sc-25637; Santa Cruz Biotechnology), mouse anti-PLK1 (05-844, clone 35-206; Millipore, Temecula, CA), Mklp1 (sc-867, Santa Cruz Biotechnology), rabbit anti–Aurora-B pT232 (Rockland, Gilbertsville, PA), rabbit Aurora-B (ab70238; Abcam), and mouse anti–α-tubulin, 1:2000 (DM1A; Sigma-Aldrich). Alexa Fluor 594– and 488–conjugated secondary antibodies (Molecular Probes, Eugene, OR) were used for primary antibody detection at 1:100. 4′,6-Diamidino-2-phenylindole was used for nucleus staining at 0.1 μg/ml (Molecular Probes). Coverslips were mounted using Prolong Antifade reagent (Molecular Probes) and imaged using

an Olympus BX-61 microscope with an ORCA-ER CCD camera (Hamamatsu, Bridgewater, NJ) and UPlanFl 40× or PlanApo 60× objective (Olympus) controlled by SlideBook (Intelligent Imaging Innovations, Denver, CO). ImageJ (National Institutes of Health, Bethesda, MD) and GIMP (www.gimp.org/) were used for image processing. Determination of midbody-stage cells was done by analysis of α-tubulin staining. Aurora-B inhibition was achieved by addition of 2 μM ZM447439 (Biomol, Plymouth, PA) 2 h before fixation as indicated.

Live cell imaging

HeLa cells stably expressing GFP-tagged histone H2B (GFP-H2B) or GFP-tagged tubulin (GFP-tubulin) were seeded on six-well plates, transfected with either control or LARG targeted siRNA at 10% confluency, and synchronized at G1/S by the double-thymidine method. After washout, cells were released for 3–4 h before being placed in a temperature-controlled chamber for filming. Bright-field and GFP images were acquired every 5 min for 24–36 h using a Nikon TE2000 microscope (Nikon, Tokyo, Japan) controlled by MetaMorph (Molecular Devices, Sunnyvale, CA). For caspase inhibition experiments, cells were treated with vehicle (DMSO) or 25 μM Z-VAD-FMK (Santa Cruz Biotechnology) immediately after washout from G1/S block. ImageJ and GIMP were used for image stack analysis and montage composition.

RhoA binding assays

LARG plasmids were transfected in HeLa cells as previously described. After 24 or 48 h of expression, cell lysates were harvested and subjected to GST-G17A-RhoA binding experiments, as described (Garcia-Mata *et al.*, 2006). Relative levels of binding to transition-state mimic RhoA were determined by comparison of LARG detected by immunoblot in pull-down fractions to input as indicated.

ACKNOWLEDGMENTS

We thank C. Fischer, L. Klayman, C. So, and J. Benovic for critical reading of the manuscript and C. Fischer for preparation of GST-G17A-RhoA. This work was supported by National Institutes of Health Grant R01 GM062884 (P.B.W.). The authors acknowledge the Imaging and Cell Culture facilities at Fox Chase Cancer Center for equipment and technical support. T.J.Y. was supported in part by National Institutes of Health Grant GM086877, National Cancer Institute core grant CA06927, Department of Defense Grant OC100172, an Appropriation from the Commonwealth of Pennsylvania, and Pennsylvania CURE. N.B was supported by the Plain and Fancy Board of Associates Fellowship, FCCC.

REFERENCES

Aittaleb M, Gao G, Evelyn CR, Neubig RR, Tesmer JJ (2009). A conserved hydrophobic surface of the LARG pleckstrin homology domain is critical for RhoA activation in cells. Cell Signal 21, 1569–1578.

Asiedu M, Wu D, Matsumura F, Wei Q (2009). Centrosome/spindle pole-associated protein regulates cytokinesis via promoting the recruitment of MyoGEF to the central spindle. Mol Biol Cell 20, 1428–1440.

Aurandt J, Vikis HG, Gutkind JS, Ahn N, Guan KL (2002). The semaphorin receptor plexin-B1 signals through a direct interaction with the Rho-specific nucleotide exchange factor, LARG. Proc Natl Acad Sci USA 99, 12085–12090.

Becknell B, Shen T, Maghraby E, Taya S, Kaibuchi K, Caligiuri MA, Marcucci G (2003). Characterization of leukemia-associated Rho guanine nucleotide exchange factor (LARG) expression during murine development. Cell Tissue Res 314, 361–366.

Bement WM, Benink HA, von Dassow G (2005). A microtubule-dependent zone of active RhoA during cleavage plane specification. J Cell Biol 170, 91–101.

Birkenfeld J (2007). GEF-H1 modulates localized RhoA activation during cytokinesis under the control of mitotic kinases. Dev Cell 12, 699–712.

Birkenfeld J, Nalbant P, Bohl BP, Pertz O, Hahn KM, Bokoch GM (2007). GEF-H1 modulates localized RhoA activation during cytokinesis under the control of mitotic kinases. Dev Cell 12, 699–712.

Chang YC, Nalbant P, Birkenfeld J, Chang ZF, Bokoch GM (2008). GEF-H1 couples nocodazole-induced microtubule disassembly to cell contractility via RhoA. Mol Biol Cell 19, 2147–2153.

Dambournet D, Machicoane M, Chesneau L, Sachse M, Rocancourt M, El Marjou A, Formstecher E, Salomon R, Goud B, Echard A (2011). Rab35 GTPase and OCRL phosphatase remodel lipids and F-actin for successful cytokinesis. Nat Cell Biol 13, 981–988.

Di Leonardo A, Khan SH, Linke SP, Greco V, Seidita G, Wahl GM (1997). DNA rereplication in the presence of mitotic spindle inhibitors in human and mouse fibroblasts lacking either p53 or pRb function. Cancer Res 57, 1013–1019.

Dubash AD, Wennerberg K, Garcia-Mata R, Menold MM, Arthur WT, Burridge K (2007). A novel role for Lsc/p115 RhoGEF and LARG in regulating RhoA activity downstream of adhesion to fibronectin. J Cell Sci 120, 3989–3998.

Eggert US, Mitchison TJ, Field CM (2006). Animal cytokinesis: from parts list to mechanisms. Annu Rev Biochem 75, 543–566.

Elia N, Sougrat R, Spurlin TA, Hurley JH, Lippincott-Schwartz J (2011). Dynamics of endosomal sorting complex required for transport (ESCRT) machinery during cytokinesis and its role in abscission. Proc Natl Acad Sci USA 108, 4846–4851.

Estey MP, Di Ciano-Oliveira C, Froese CD, Bejide MT, Trimble WS (2010). Distinct roles of septins in cytokinesis: SEPT9 mediates midbody abscission. J Cell Biol 191, 741–749.

Evelyn CR, Ferng T, Rojas RJ, Larsen MJ, Sondek J, Neubig RR (2009). High-throughput screening for small-molecule inhibitors of LARG-stimulated RhoA nucleotide binding via a novel fluorescence polarization assay. J Biomol Screen 14, 161–172.

Fededa JP, Gerlich DW (2012). Molecular control of animal cell cytokinesis. Nat Cell Biol 14, 440–447.

Fujishiro SH, Tanimura S, Mure S, Kashimoto Y, Watanabe K, Kohno M (2008). ERK1/2 phosphorylate GEF-H1 to enhance its guanine nucleotide exchange activity toward RhoA. Biochem Biophys Res Commun 368, 162–167.

Fujiwara T (2005). Cytokinesis failure generating tetraploids promotes tumorigenesis in p53-null cells. Nature 437, 1043–1047.

Fukuhara S, Chikumi H, Gutkind JS (2000). Leukemia-associated Rho guanine nucleotide exchange factor (LARG) links heterotrimeric G proteins of the G(12) family to Rho. FEBS Lett 485, 183–188.

Gai M, Camera P, Dema A, Bianchi F, Berto G, Scarpa E, Germena G, Di Cunto F (2011). Citron kinase controls abscission through RhoA and anillin. Mol Biol Cell 22, 3768–3778.

Garcia-Mata R, Wennerberg K, Arthur WT, Noren NK, Ellerbroek SM, Burridge K (2006). Analysis of activated GAPs and GEFs in cell lysates. Methods Enzymol 406, 425–437.

Goulimari P, Knieling H, Engel U, Grosse R (2008). LARG and mDia1 link Galpha12/13 to cell polarity and microtubule dynamics. Mol Biol Cell 19, 30–40.

Grabocka E, Wedegaertner PB (2007). Disruption of oligomerization induces nucleocytoplasmic shuttling of leukemia-associated Rho guanine-nucleotide exchange factor. Mol Pharmacol 72, 993–1002.

Gromley A (2005). Centriolin anchoring of exocyst and SNARE complexes at the midbody is required for secretory-vesicle-mediated abscission. Cell 123, 75–87.

Guilluy C, Swaminathan V, Garcia-Mata R, O'Brien ET, Superfine R, Burridge K (2011). The Rho GEFs LARG and GEF-H1 regulate the mechanical response to force on integrins. Nat Cell Biol 13, 722–727.

Huang H-C, Shi J, Orth JD, Mitchison TJ (2009). Evidence that mitotic exit is a better cancer therapeutic target than spindle assembly. Cancer Cell 16, 347–358.

Kanda T, Sullivan KF, Wahl GM (1998). Histone-GFP fusion protein enables sensitive analysis of chromosome dynamics in living mammalian cells. Curr Biol 8, 377–385.

Kerr JF, Wyllie AH, Currie AR (1972). Apoptosis: a basic biological phenomenon with wide-ranging implications in tissue kinetics. Br J Cancer 26, 239–257.

Kitzing TM, Sahadevan AS, Brandt DT, Knieling H, Hannemann S, Fackler OT, Grosshans J, Grosse R (2007). Positive feedback between Dia1, LARG, and RhoA regulates cell morphology and invasion. Genes Dev 21, 1478–1483.

Krendel M, Zenke FT, Bokoch GM (2002). Nucleotide exchange factor GEF-H1 mediates cross-talk between microtubules and the actin cytoskeleton. Nat Cell Biol 4, 294–301.
Kristelly R, Earnest BT, Krishnamoorthy L, Tesmer JJG (2003). Preliminary structure analysis of the DH/PH domains of leukemia-associated RhoGEF. Acta Crystallogr D 59, 1859–1862.
Loria A, Longhini KM, Glotzer M (2012). The RhoGAP domain of CYK-4 has an essential role in RhoA activation. Curr Biol 22, 213–219.
Mackay DR, Makise M, Ullman KS (2010). Defects in nuclear pore assembly lead to activation of an Aurora B-mediated abscission checkpoint. J Cell Biol 191, 923–931.
Matuliene J, Kuriyama R (2002). Kinesin-like protein CHO1 is required for the formation of midbody matrix and the completion of cytokinesis in mammalian cells. Mol Biol Cell 13, 1832–1845.
Medlin MD, Staus DP, Dubash AD, Taylor JM, Mack CP (2010). Sphingosine 1-phosphate receptor 2 signals through leukemia-associated RhoGEF (LARG), to promote smooth muscle cell differentiation. Arterioscler Thromb Vasc Biol 30, 1779–1786.
Mishima M, Kaitna S, Glotzer M (2002). Central spindle assembly and cytokinesis require a kinesin-like protein/RhoGAP complex with microtubule bundling activity. Dev Cell 2, 41–54.
Mullins J, Biesele J (1977). Terminal phase of cytokinesis in D-98S cells. J Cell Biol 73, 672–684.
Neto H, Gould GW (2011). The regulation of abscission by multi-protein complexes. J Cell Sci 124, 3199–3207.
Nishimura Y, Yonemura S (2006). Centralspindlin regulates ECT2 and RhoA accumulation at the equatorial cortex during cytokinesis. J Cell Sci 119, 104–114.
Norden C, Mendoza M, Dobbelaere J, Kotwaliwale CV, Biggins S, Barral Y (2006). The NoCut pathway links completion of cytokinesis to spindle midzone function to prevent chromosome breakage. Cell 125, 85–98.
Perrot V, Vazquez-Prado J, Gutkind JS (2002). Plexin B regulates Rho through the guanine nucleotide exchange factors leukemia-associated Rho GEF (LARG) and PDZ-RhoGEF. J Biol Chem 277, 43115–43120.
Petronczki M, Glotzer M, Kraut N, Peters JM (2007). Polo-like kinase 1 triggers the initiation of cytokinesis in human cells by promoting recruitment of the RhoGEF Ect2 to the central spindle. Dev Cell 12, 713–725.
Pfreimer M, Vatter P, Langer T, Wieland T, Gierschik P, Moepps B (2012). LARG links histamine-H1-receptor-activated Gq to Rho-GTPase-dependent signaling pathways. Cell Signal 24, 652–663.
Pohl C, Jentsch S (2008). Final stages of cytokinesis and midbody ring formation are controlled by BRUCE. Cell 132, 832–845.
Rieder CL, Palazzo RE (1992). Colcemid and the mitotic cycle. J Cell Sci 102, (Pt 3), 387–392.
Shi Y, Zhang J, Mullin M, Dong B, Alberts AS, Siminovitch KA (2009). The mDial formin is required for neutrophil polarization, migration, and activation of the LARG/RhoA/ROCK signaling axis during chemotaxis. J Immunol 182, 3837–3845.
Slee EA, Adrain C, Martin SJ (2001). Executioner caspase-3, -6, and -7 perform distinct, non-redundant roles during the demolition phase of apoptosis. J Biol Chem 276, 7320–7326.
Steigemann P (2009). Aurora B-mediated abscission checkpoint protects against tetraploidization. Cell 136, 473–484.
Steigemann P, Gerlich DW (2009). Cytokinetic abscission: cellular dynamics at the midbody. Trends Cell Biol 19, 606–616.
Steigemann P, Wurzenberger C, Schmitz MH, Held M, Guizetti J, Maar S, Gerlich DW (2009). Aurora B-mediated abscission checkpoint protects against tetraploidization. Cell 136, 473–484.
Su K-C, Takaki T, Petronczki M (2011a). Targeting of the RhoGEF Ect2 to the equatorial membrane controls cleavage furrow formation during cytokinesis. Dev Cell 21, 1104–1115.
Su KC, Takaki T, Petronczki M (2011b). Targeting of the RhoGEF Ect2 to the equatorial membrane controls cleavage furrow formation during cytokinesis. Dev Cell 21, 1104–1115.
Suzuki N, Tokita R, Minami S (2007). Involvement of IGF-1/LARG signaling in the differentiation of neural stem cells into oligodendrocytes. J Nippon Med Sch 47, 3–2.
Swiercz JM, Kuner R, Behrens J, Offermanns S (2002). Plexin-B1 directly interacts with PDZ-RhoGEF/LARG to regulate RhoA and growth cone morphology. Neuron 35, 51–63.
Tao W, South VJ, Zhang Y, Davide JP, Farrell L, Kohl NE, Sepp-Lorenzino L, Lobell RB (2005). Induction of apoptosis by an inhibitor of the mitotic kinesin KSP requires both activation of the spindle assembly checkpoint and mitotic slippage. Cancer Cell 8, 49–59.
Tatsumoto T, Xie X, Blumenthal R, Okamoto I, Miki T (1999). Human Ect2 is an exchange factor for Rho GTPases, phosphorylated in G2/M phases, and involved in cytokinesis. J Cell Biol 147, 921–928.
Tomas A (2004). Annexin 11 is required for midbody formation and completion of the terminal phase of cytokinesis. J Cell Biol 165, 813–822.
Wolfe BA, Takaki T, Petronczki M, Glotzer M (2009). Polo-like kinase 1 directs assembly of the HsCyk-4 RhoGAP/Ect2 RhoGEF complex to initiate cleavage furrow formation. PLoS Biol 7, e1000110.
Wu D, Asiedu M, Adelstein RS, Wei Q (2006). A novel guanine nucleotide exchange factor MyoGEF is required for cytokinesis. Cell Cycle 5, 1234–1239.
Yang D (2008). Structural basis for midbody targeting of spastin by the ESCRT-III protein CHMP1B. Nat Struct Mol Biol 15, 1278–1286.
Yonemura S, Hirao-Minakuchi K, Nishimura Y (2004). Rho localization in cells and tissues. Exp Cell Res 295, 300–314.
Yüce O, Piekny A, Glotzer M (2005). An ECT2–centralspindlin complex regulates the localization and function of RhoA. J Cell Biol 170, 571–582.